

Nematicity as a Probe of Superconducting Pairing in Iron-Based Superconductors

Rafael M. Fernandes^{1,*} and Andrew J. Millis²

¹*School of Physics and Astronomy, University of Minnesota, Minneapolis, Minnesota 55455, USA*

²*Department of Physics, Columbia University, New York, New York 10027, USA*

(Received 6 June 2013; published 16 September 2013)

In several families of iron-based superconducting materials, a d -wave pairing instability may compete with the leading s -wave instability. Here, we show that when both states have comparable free energies, superconducting and nematic degrees of freedom are strongly coupled. Whereas nematic order causes a sharp nonanalytic increase in T_c , nematic fluctuations can change the character of the s -wave to d -wave transition, favoring an intermediate state that does not break time-reversal symmetry but does break tetragonal symmetry. The coupling between superconductivity and nematicity is also manifested in the strong softening of the shear modulus across the superconducting transition. Our results show that nematicity can be used as a diagnostic tool to search for unconventional pairing states in iron pnictides and chalcogenides.

DOI: 10.1103/PhysRevLett.111.127001

PACS numbers: 74.70.Xa, 74.20.Mn, 74.20.Rp, 74.62.-c

Two of the main themes in the current studies of iron-based superconductors are the possibility of unconventional forms of superconducting (SC) pairing [1] [most likely mediated by spin fluctuations [2]] and the importance of electronic nematic degrees of freedom [3–7]. Pairing interactions mediated by spin fluctuations promote both s^{+-} and d -wave superconducting instabilities, with the former typically winning over the latter [8–12]. The same spin fluctuations [7], possibly combined with orbital degrees of freedom [13–16], can give rise to an emergent electronically driven breaking of rotational symmetry [17–19], often referred to as nematic order [20]. The interplay between s^{+-} and d -wave superconductivity has been extensively studied [8–10,12,21–23] as has the interplay between s^{+-} and nematic order [24–27], but the coupling of all three seems not to have previously been considered. Here, we show that such a coupling can have dramatic effects, qualitatively changing the phase diagram, increasing the SC transition temperature T_c , and helping to distinguish an s - d competition from other proposed phases.

Whereas in most iron-based superconductors the pairing state is believed to be s^{+-} , both theoretical and experimental work suggests that a d -wave state may be near in free energy or even actually occur. In particular, in $(\text{Ba}_{1-x}\text{K}_x)\text{Fe}_2\text{As}_2$ and $\text{Ba}(\text{Fe}_{1-x}\text{Mn}_x)_2\text{As}_2$ pnictides and $A_{1-y}\text{Fe}_{2-x}\text{Se}_2$ chalcogenides (see Fig. 1), calculations indicate that the d -wave state may be tuned by varying the pnictogen height [28], the p - d orbital hybridization [29], applied pressure [30], and strength of Néel fluctuations [23]. Near the point where the s and d wave states cross in free energy, a time-reversal symmetry-breaking (TRSB) $s + id$ state has been predicted [21,31]. The experimental situation is not settled: in $(\text{Ba}_{1-x}\text{K}_x)\text{Fe}_2\text{As}_2$ the consensus is that at optimal doping ($x \approx 0.4$) the state is fully gapped and of s symmetry [32] whereas in the $x = 1$ compound thermal conductivity [33] and angle resolved

photoemission spectroscopy (ARPES) measurements [34] favor respectively a d -wave and a nodal s^{+-} state. In $A_{1-y}\text{Fe}_{2-x}\text{Se}_2$, inelastic neutron scattering [35] favors a d -wave state whereas ARPES indicates a nodeless s -wave state [36]. In the hole-doped $\text{Ba}(\text{Fe}_{1-x}\text{Mn}_x)_2\text{As}_2$, neutron scattering finds both Néel and stripe-type magnetic

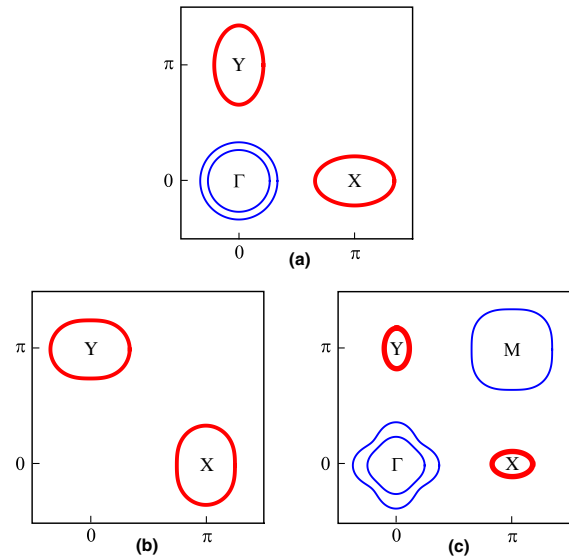


FIG. 1 (color online). Schematic Fermi surfaces of three different systems where competing s^{+-} and d -wave instabilities have been proposed [21–23,28,29,50]. Thick red (thin blue) lines denote electron (hole) pockets. (a) In $\text{Ba}(\text{Fe}_{1-x}\text{Mn}_x)_2\text{As}_2$, the s^{+-} state arises from $(\pi, 0)/(0, \pi)$ stripe-type fluctuations, whereas the d -wave state comes from (π, π) Néel-type fluctuations [23]. (b) In $A_{1-y}\text{Fe}_{2-x}\text{Se}_2$ chalcogenides, a d -wave state appears due to the direct XY interaction [50], whereas s^{+-} is favored by FeAs hybridization [29]. (c) In strongly doped $(\text{Ba}_{1-x}\text{K}_x)\text{Fe}_2\text{As}_2$, the s^{+-} state appears when small electron pockets emerge with doping, whereas a d -wave state can appear due to the M intrapocket interaction [22,28].

fluctuations [37], which favor d - and s -wave states, respectively, but no superconductivity has been observed. Raman scattering [38] in some of these materials indicates the existence of a Bardasis-Schrieffer mode, suggesting the presence of two competing SC instabilities. The unsettled experimental situation along with the compelling theoretical reasons to expect a proximal d -wave state motivates a more detailed examination of the physics associated with a change from s to d symmetry.

The change from s^{+-} to d -wave superconductivity in the absence of nematicity [21,31] and the interplay between nematicity and a single SC order parameter [24–26] have been studied. On general grounds, one expects that a single superconducting order parameter Δ couples to a nematic order parameter φ via the biquadratic term $\Delta^2\varphi^2$ in the free energy [27]. This coupling leads to a suppression of superconductivity in the presence of nematicity and vice versa as well as to a hardening of the shear modulus below T_c . These features have been reported in the $\text{Ba}(\text{Fe}_{1-x}\text{Co}_x)_2\text{As}_2$ materials [19,24].

The key new aspect of our analysis is that if both s - and d -symmetry superconductivity are important, then the free energy will contain also a trilinear term

$$F_{\text{SC-nem}} \propto \varphi \Delta_s \Delta_d \cos\theta \quad (1)$$

connecting the s -wave, d -wave, and nematic order parameters (here θ is the relative phase of the two SC order parameters). As we shall show, this coupling implies that (1) nematic order leads to an enhancement of the SC transition temperature; (2) superconductivity can lead to the appearance of a nematic phase; (3) an $s + d$ symmetry phase [similar to the one proposed in Ref. [39]] or a first-order transition can separate the pure s^{+-} and d -wave states; and (4) a softening of the shear modulus below T_c is an experimental signature of proximity to the regime where s^{+-} and d -wave SC states are degenerate.

These results are robust and do not rely on any specific shape of the Fermi surface, as they follow from a general Ginzburg-Landau analysis based on a free energy that respects the gauge and rotational symmetries of the system

$$F = F_{\text{nem}}(\varphi^2) + \frac{t_s}{2} \Delta_s^2 + \frac{t_d}{2} \Delta_d^2 + \frac{\beta_s}{4} \Delta_s^4 + \frac{\beta_d}{4} \Delta_d^4 + \frac{1}{2} \Delta_s^2 \Delta_d^2 (\beta_{sd} + \alpha \cos 2\theta) + \lambda \varphi \Delta_s \Delta_d \cos\theta. \quad (2)$$

Here, F_{nem} is the free energy of the pure nematic phase, $t_j = a_j(T - T_{c,j})$ with $a_j > 0$ gives the distance to the SC transition temperatures in the $j = s^{+-}, d$ channels, and λ , α , and the β_i are coupling constants. Note that the biquadratic couplings $\Delta_{s/d}^2 \varphi^2$ are subleading near the s - d transition and are not written explicitly here. In the materials discussed above, $T_{c,s}$ and $T_{c,d}$ are tuned by the doping concentration x due to different mechanisms: In $\text{Ba}(\text{Fe}_{1-x}\text{Mn}_x)_2\text{As}_2$ [Fig. 1(a)], increasing x leads to stronger Néel fluctuations, which favor the d -wave state [23]. In $\text{A}_{1-y}\text{Fe}_{2-x}\text{Se}_2$ [Fig. 1(b)], changing x modifies the Fe-As hybridization, which in turn favors either s -wave or d -wave state [29]. In $(\text{Ba}_{1-x}\text{K}_x)\text{Fe}_2\text{As}_2$ [Fig. 1(c)],

increasing x gives rise to a large hole pocket at the M point, which favors a d -wave state [22,28]. For illustration, in the Supplemental Material [40] we derive this free energy from a BCS model appropriate for the system in Fig. 1(a), but we emphasize that our conclusions are more general.

In the absence of significant nematicity, we find $\alpha > 0$, implying that the free energy is minimized by setting $\theta = \pi/2$. We also find that $(\beta_{sd} - |\alpha|)^2 < \beta_s \beta_d$, implying that the s -wave and d -wave states can be simultaneously present [41]. In this case, near the degeneracy point $T_{c,s} = T_{c,d} = T^*$, the two order parameters enter in the form $s + id$, breaking time-reversal symmetry. Note that microscopic models also found $s + id$ states in systems with the Fermi surfaces of Figs. 1(b) and 1(c) [28,29]. The resulting phase diagram in the absence of nematicity is shown schematically in Fig. 2(a).

Including nematicity leads to significant changes. Consider first the case that a nematic phase transition

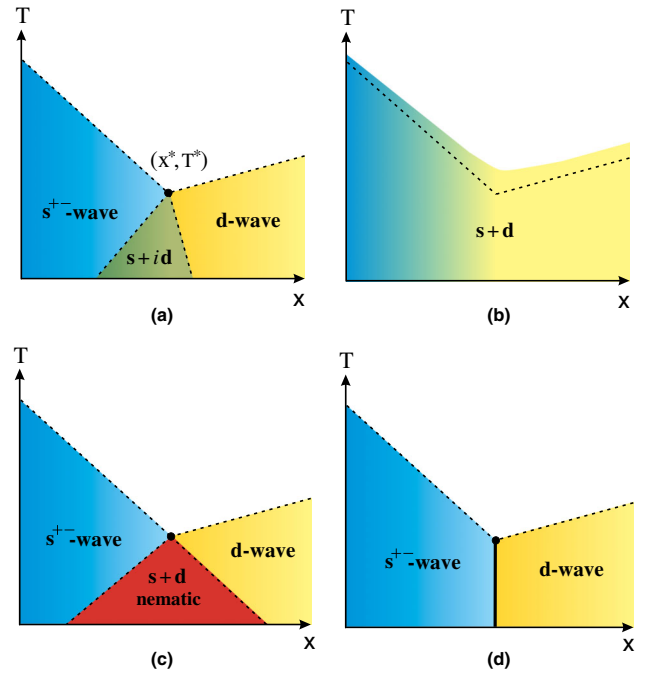


FIG. 2 (color online). Schematic phase diagrams as function of temperature (T) and doping (x) for the interplay between s^{+-} -wave and d -wave superconductivity in iron pnictide materials. Dotted (solid) lines denote second- (first-) order phase transitions. Panel (a): no nematic order and weak nematic fluctuations ($\chi_{\text{nem}} < 2\alpha/\lambda^2$). The s -wave and d -wave states are separated by an intermediate TRSB $s + id$ state. Panel (b): preexisting nematic order. T_c is enhanced with respect to the tetragonal case (dashed line), and the superconducting order parameter is characterized by the real combination $s + d$ and evolves smoothly with x with no TRSB. Panel (c): no nematic order, but larger nematic fluctuations ($2\alpha < \lambda^2 \chi_{\text{nem}} < \beta_{sd} + \alpha + \sqrt{\beta_s \beta_d}$). The coexistence region is enhanced, but the intermediate state is of $s + d$ character, spontaneously breaking rotational but not time-reversal symmetry. Panel (d): no nematic order, but even larger nematic fluctuations ($\lambda^2 \chi_{\text{nem}} > \beta_{sd} + \alpha + \sqrt{\beta_s \beta_d}$). The s -wave to d -wave transition becomes first order.

occurs at a temperature far above the SC transition temperature. In this case, extremizing F_{nem} leads to a nonzero expectation value of the nematic order parameter $\langle \varphi \rangle = \varphi_0$ so the SC free energy contains an effective bilinear term $\lambda \varphi_0 \Delta_s \Delta_d \cos \theta$. Diagonalizing the quadratic part of the free energy reveals that the energy minimum is at $\theta = 0$, so the SC order parameter becomes a real admixture of s - and d -wave gaps, evolving smoothly across the degeneracy point (see Supplemental Material [40]). T_c , determined from the solution of $t_c t_d = \lambda^2 \varphi_0^2$, is enhanced relative to its tetragonal value $T_{c,s/d}$, with the enhancement being largest at the degeneracy point $T_{c,s} = T_{c,d} = T^*$ where we find the nonanalytic behavior $T_c - T^* \propto |\varphi_0|$ and the maximal admixture between s -wave and d -wave states. Away from this point, $T_c - T_{c,s/d} \propto \varphi_0^2$. Figure 2(b) shows the phase diagram corresponding to this situation. We note that if the coupling λ is not too strong, an $s + id$ phase may appear at lower temperatures [42].

We now consider that nematic order is absent but nematic fluctuations are important. In this case, we approximate $F_{\text{nem}} = (1/2) \chi_{\text{nem}}^{-1} \varphi^2$, where χ_{nem} is the nematic susceptibility that would diverge at the nematic transition. Minimizing with respect to the nematic order parameter, we find $\varphi = -\lambda \chi_{\text{nem}} \Delta_s \Delta_d \cos \theta$. Substituting back into Eq. (2) yields

$$\begin{aligned} \tilde{F} = & \frac{t_s}{2} \Delta_s^2 + \frac{t_d}{2} \Delta_d^2 + \frac{\beta_s}{4} \Delta_s^4 + \frac{\beta_d}{4} \Delta_d^4 \\ & + \frac{1}{2} \Delta_s^2 \Delta_d^2 (\tilde{\beta}_{sd} + \tilde{\alpha} \cos 2\theta) \end{aligned} \quad (3)$$

with $\tilde{\alpha} = \alpha - (1/2) \lambda^2 \chi_{\text{nem}}$ and $\tilde{\beta}_{sd} = \beta_{sd} - (1/2) \lambda^2 \chi_{\text{nem}}$. For weak nematic fluctuations $\chi_{\text{nem}} < 2\alpha/\lambda^2$, $\tilde{\alpha}$ remains positive and the relative phase remains at $\theta = \pi/2$ so that the phase diagram retains the form displayed in Fig. 2(a), with $\varphi = 0$.

As the nematic instability is approached, χ_{nem} increases and eventually $\tilde{\alpha}$ changes sign so that the energy minimum shifts from $\theta = \pi/2$ to $\theta = 0, \pi$. Note that the BCS calculations, which indicate that $\alpha < \beta_{sd}$, imply that the sign change in $\tilde{\alpha}$ happens before the condition for a second-order phase transition is violated. Consequently, the SC state takes the real form $s \pm d$ and the nematic order parameter acquires a nonvanishing expectation value $\varphi = \pm \lambda \chi_{\text{nem}} \Delta_s \Delta_d$ indicating a spontaneous breaking of tetragonal symmetry as shown in Fig. 2(c). Note that an $s \pm d$ state was also found in the $T = 0$ numerical results of Ref. [39]. As the nematic susceptibility further increases, $\tilde{\beta}_{sd}$ changes sign and eventually the magnitude of $(\tilde{\beta}_{sd} - |\tilde{\alpha}|)^2$ becomes large enough that the transition between s and d becomes first order as shown in Fig. 2(d). An estimate for the critical nematic susceptibility above which $s \pm d$ emerges reveals that it corresponds to moderate fluctuations that are reasonable to be expected in the real materials [see Supplemental Material [40]]. In this regard, note that shear modulus measurements have revealed the presence of significant nematic fluctuations in the phase diagrams of 122 compounds [19,43].

The analysis so far has been based only on symmetry arguments, but it is of interest to demonstrate a mechanism and provide an estimate for the magnitude of the effect. We present a spin fluctuation Eliashberg calculation following Ref. [23] but including nematicity, for the system whose Fermi surface is displayed in Fig. 1(a), with hole pockets at the center of the Brillouin zone $\Gamma = (0, 0)$ and electron pockets centered at $X = (\pi, 0)$ and $Y = (0, \pi)$. Stripe spin fluctuations [peaked at $\mathbf{Q}_X = (\pi, 0)$ and $\mathbf{Q}_Y = (0, \pi)$] induce repulsive Γ - X and Γ - Y interactions that favor an s^{+-} state, whereas Néel fluctuations [peaked at $\mathbf{Q}_N = (\pi, \pi)$] induce a repulsive X - Y interaction that favors a d -wave state [23].

In the Eliashberg formalism, the pairing interactions are determined by the dynamic magnetic susceptibilities $\chi_i(\mathbf{Q}_i + \mathbf{q}, \omega)$ with $i = X, Y, N$ [see Supplemental Material for more details [40]]. Neutron scattering experiments reveal that all of the relevant spin fluctuations are overdamped [37], $\chi_i^{-1}(\mathbf{Q}_i + \mathbf{q}, \omega) = \xi_i^{-2} + q^2 - i\omega\gamma_i^{-1}$, and are characterized by two parameters: the magnetic correlation length ξ_i and the Landau damping γ_i . As we have previously shown [23], in the tetragonal phase where $\xi_X = \xi_Y = \xi_S$ the system undergoes a transition from an s^{+-} to a d -wave SC state as the Néel correlation length ξ_N increases from zero [see Fig. 3(a)].

In the presence of long-range nematic order, tetragonal symmetry is broken and the two stripe-type correlation lengths ξ_X and ξ_Y become different, with $\varphi = \ln(\xi_X/\xi_Y)$ [7], implying that the pairing interaction is different between the Γ - X and Γ - Y pockets. In Fig. 3(a), we show the numerically calculated T_c in the nematic phase. We observe a behavior similar to the schematic phase diagram of Fig. 2(b), with the maximum relative increase of T_c at the s -wave/ d -wave degeneracy point $\xi_N \approx 0.33\xi_S$. Far from this point, T_c decreases as φ^2 for increasing nematic order, reflecting the usual competing biquadratic coupling

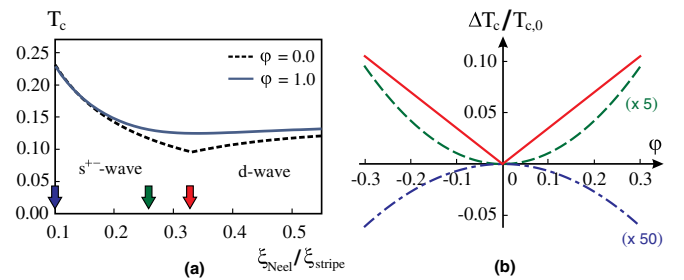


FIG. 3 (color online). Dependence of T_c on the Néel-type ($\xi_{\text{Néel}}$) and stripe-type (ξ_{stripe}) magnetic correlation lengths obtained from Eliashberg calculations as described in the text. Panel (a) shows the evolution of T_c (in units of $\gamma_{\text{stripe}}/2\pi$) as function of $\xi_{\text{Néel}}/\xi_{\text{stripe}}$ in the absence (dashed line) and presence of nematic order (solid line, $\varphi = 1.0$). Panel (b) presents the variation of T_c , $\Delta T_c = T_c - T_{c,0}$, as function of the nematic order parameter $\varphi = \ln(\xi_X/\xi_Y)$, for three fixed values of the ratio $\xi_{\text{Néel}}/\xi_{\text{stripe}}$ indicated by the arrows in panel (a): $\xi_{\text{Néel}}/\xi_{\text{stripe}} = 0.1$ (dot-dashed blue line), $\xi_{\text{Néel}}/\xi_{\text{stripe}} = 0.26$ (dashed green line), and $\xi_{\text{Néel}}/\xi_{\text{stripe}} = 0.33$ (solid red line).

$\varphi^2 \Delta_s^2$ between orders that break different symmetries [Fig. 3(b)]. As the degeneracy point is approached, the d -wave instability becomes closer in energy to the s^{+-} one, and T_c starts to increase with increasing nematic order as φ^2 . In the vicinities of the degeneracy point, this behavior changes and we observe the increase of T_c with $|\varphi|$, a signature of the trilinear coupling (1), as discussed within the Ginzburg-Landau model. From our numerical results, we can estimate the coupling constant $\lambda \approx 0.33$; i.e., making $\xi_X \approx 1.35 \xi_Y$ leads to a 10% enhancement of the relative transition temperature $(T_c - T_{c,0})/T_{c,0}$.

Measurements of elastic anomalies across the superconducting transition can also reveal the strength of the trilinear coupling. The idea, which goes back to the work of Testardi and others on the A-15 materials [44] and was revisited in the context of the cuprates [45], is that within mean field theory, as the temperature is decreased below T_c , the free energy acquires an additional contribution

$$\Delta F = -\frac{1}{2} \frac{\Delta C}{T_c} [T - T_c(\varphi)]^2. \quad (4)$$

Here, ΔC is the specific heat jump across the transition. The crucial point is that the dependence of T_c on the strain (proportional to φ) leads to new contributions to the elastic free energy that are singular at T_c and proportional to the strain derivatives of T_c and to ΔC . Differentiating Eq. (4) twice with respect to strain and retaining only the most singular terms at T_c gives discontinuities in the shear elastic modulus C_{66} and its first temperature derivative

$$\Delta C_{66} \equiv C_{66}(T_c^-) - C_{66}(T_c^+) = -\frac{\Delta C}{T_c} \left(\frac{\partial T_c}{\partial \varphi} \right)^2, \quad (5)$$

$$\Delta \frac{dC_{66}}{dT} = \frac{\Delta C}{T_c} \frac{\partial^2 T_c}{\partial \varphi^2}. \quad (6)$$

In the nematic phase or at the $s-d$ degeneracy point in Fig. 2(c), because T_c depends linearly on φ , the elastic modulus exhibits a downwards jump (softening) across T_c . In the tetragonal phase, T_c depends quadratically on φ . Far from the $s-d$ degeneracy point, the $\varphi^2 \Delta^2$ free energy term discussed in Refs. [24,27]—present in the Eliashberg calculations but not explicitly written in Eq. (2)—gives a negative $\partial^2 T_c / \partial \varphi^2$ [see Fig. 3(b)]. This implies a hardening of C_{66} below T_c , as observed in optimally doped $\text{Ba}(\text{Fe}_{1-x}\text{Co}_x)_2\text{As}_2$ [19,43]. However, as the d -wave state is approached, the trilinear coupling leads to a positive contribution λ^2/t_d to $\partial^2 T_c / \partial \varphi^2$, which diverges at the degeneracy point, causing a softening in C_{66} . A softening of C_{66} across T_c is thus a clear signal of proximity between s -wave and d -wave states.

Compounds to which the considerations of this Letter may be relevant include $\text{A}_{1-y}\text{Fe}_{2-x}\text{Se}_2$ chalcogenides, where neutron scattering [35] and ARPES [36] seem to support different pairing states, and KFe_2As_2 , where experiment suggests a change in pairing state with applied pressure [46]. Furthermore, in the optimally doped compound $\text{BaFe}_2(\text{As}_{1-x}\text{P}_x)_2$, recent detwinning experiments found an unexpected enhancement of T_c with the applied strain [47], as expected if the trilinear coupling is relevant.

The results here may also help to resolve a controversy concerning the superconducting state of the extremely overdoped pnictide compound $(\text{Ba}_{1-x}\text{K}_x)\text{Fe}_2\text{As}_2$, which is believed to possess the Fermi surface shown in Fig. 1(c). ARPES experiments [34] support a scenario where the SC state evolves from nodeless s^{+-} at optimal doping $x_{\text{opt}} \approx 0.4$ towards nodal s^{+-} at $x = 1$ [with a possible intermediate TRSB $s + is$ state [42]]. Thermal conductivity measurements [33] support a transition from nodeless s^{+-} at x_{opt} to d wave at $x = 1$. Calculations [12,22] indicate that the two states have comparable transition temperatures. The results of this Letter indicate that if the second state is d wave then a structural/nematic “dome,” detectable by x-ray [24] or torque magnetometry [6], could appear in the vicinity of the critical x . Also, application of a stress field to induce long-range nematic order [5] would cause a linear increase in T_c . A softening of the elastic modulus across the transition would further support a d -wave state.

In summary, our results unveil a unique feature of the interplay between nematicity and SC in iron-based materials. The trilinear coupling (1) shows that at the same time that the d -wave and s -wave gaps work together as an effective field conjugate to the nematic order parameter, allowing for spontaneous tetragonal symmetry breaking in the superconducting state, nematicity leads to an effective attraction between the two otherwise competing states. This physics can also be expected in other situations where multiple SC instabilities are present, such as the ruthenates Sr_2RuO_4 , where a chiral triplet $p + ip$ state has been proposed, and the consequences for the elastic modulus discontinuities of trilinear coupling $\varphi p_x p_y$ have been discussed [48,49].

We thank A. Chubukov, E. Fradkin, S. Maiti, C. Meingast, J. Schmalian, and L. Taillefer for inspiring discussions. A. J. M. was supported by NSF DMR 1006282.

*rfernand@umn.edu

- [1] I. I. Mazin, D. J. Singh, M. D. Johannes, and M. H. Du, *Phys. Rev. Lett.* **101**, 057003 (2008); A. V. Chubukov, D. V. Efremov, and I. Eremin, *Phys. Rev. B* **78**, 134512 (2008); K. Kuroki, S. Onari, R. Arita, H. Usui, Y. Tanaka, H. Kontani, and H. Aoki, *Phys. Rev. Lett.* **101**, 087004 (2008); V. Cvetković and Z. Tesanović, *Phys. Rev. B* **80**, 024512 (2009); J. Zhang, R. Sknepnek, R. M. Fernandes, and J. Schmalian, *Phys. Rev. B* **79**, 220502(R) (2009); A. F. Kemper, T. A. Maier, S. Graser, H.-P. Cheng, P. J. Hirschfeld, and D. J. Scalapino, *New J. Phys.* **12**, 073030 (2010).
- [2] P. J. Hirschfeld, M. M. Korshunov, and I. I. Mazin, *Rep. Prog. Phys.* **74**, 124508 (2011); A. V. Chubukov, *Annu. Rev. Condens. Matter Phys.* **3**, 57 (2012).
- [3] J.-H. Chu, J. G. Analytis, K. De Greve, P. L. McMahon, Z. Islam, Y. Yamamoto, and I. R. Fisher, *Science* **329**, 824 (2010).
- [4] M. Yi, D. Lu, J.-H. Chu, J. G. Analytis, A. P. Sorini, A. F. Kemper, B. Moritz, S.-K. Mo, R. G. Moore, M. Hashimoto, W. S. Lee, Z. Hussain, T. P. Devereaux,

- I. R. Fisher, and Z.-X. Shen, *Proc. Natl. Acad. Sci. U.S.A.* **108**, 6878 (2011).
- [5] J.-H. Chu, H.-H. Kuo, J.G. Analytis, and I.R. Fisher, *Science* **337**, 710 (2012).
- [6] S. Kasahara, H.J. Shi, K. Hashimoto, S. Tonegawa, Y. Mizukami, T. Shibauchi, K. Sugimoto, T. Fukuda, T. Terashima, A.H. Nevidomskyy, and Y. Matsuda, *Nature (London)* **486**, 382 (2012).
- [7] R.M. Fernandes, A.V. Chubukov, J. Knolle, I. Eremin, and J. Schmalian, *Phys. Rev. B* **85**, 024534 (2012).
- [8] K. Kuroki, H. Usui, S. Onari, R. Arita, and H. Aoki, *Phys. Rev. B* **79**, 224511 (2009).
- [9] S. Graser, A.F. Kemper, T.A. Maier, H.-P. Cheng, P.J. Hirschfeld, and D.J. Scalapino, *Phys. Rev. B* **81**, 214503 (2010).
- [10] S. Maiti, M.M. Korshunov, T.A. Maier, P.J. Hirschfeld, and A.V. Chubukov, *Phys. Rev. B* **84**, 224505 (2011); S. Maiti, M.M. Korshunov, T.A. Maier, P.J. Hirschfeld, and A.V. Chubukov, *Phys. Rev. Lett.* **107**, 147002 (2011).
- [11] F. Yang, F. Wang, and D.-H. Lee, [arXiv:1305.0605](https://arxiv.org/abs/1305.0605).
- [12] R. Thomale, C. Platt, W. Hanke, J. Hu, and B.A. Bernevig, *Phys. Rev. Lett.* **107**, 117001 (2011).
- [13] C.C. Lee, W.G. Yin, and W. Ku, *Phys. Rev. Lett.* **103**, 267001 (2009).
- [14] C.-C. Chen, J. Maciejko, A.P. Sorini, B. Moritz, R.R.P. Singh, and T.P. Devereaux, *Phys. Rev. B* **82**, 100504 (2010).
- [15] W.-C. Lee and P.W. Phillips, *Phys. Rev. B* **86**, 245113 (2012).
- [16] S. Onari and H. Kontani, *Phys. Rev. Lett.* **109**, 137001 (2012).
- [17] C. Fang, H. Yao, W.-F. Tsai, J.P. Hu, and S.A. Kivelson, *Phys. Rev. B* **77**, 224509 (2008).
- [18] C. Xu, M. Muller, and S. Sachdev, *Phys. Rev. B* **78**, 020501(R) (2008).
- [19] R.M. Fernandes, L.H. VanBebber, S. Bhattacharya, P. Chandra, V. Keppens, D. Mandrus, M.A. McGuire, B.C. Sales, A.S. Sefat, and J. Schmalian, *Phys. Rev. Lett.* **105**, 157003 (2010).
- [20] E. Fradkin, S.A. Kivelson, M.J. Lawler, J.P. Eisenstein, and A.P. Mackenzie, *Annu. Rev. Condens. Matter Phys.* **1**, 153 (2010).
- [21] W.-C. Lee, S.-C. Zhang, and C. Wu, *Phys. Rev. Lett.* **102**, 217002 (2009).
- [22] S. Maiti, M.M. Korshunov, and A.V. Chubukov, *Phys. Rev. B* **85**, 014511 (2012).
- [23] R.M. Fernandes and A.J. Millis, *Phys. Rev. Lett.* **110**, 117004 (2013).
- [24] S. Nandi, M.G. Kim, A. Kreyssig, R.M. Fernandes, D.K. Pratt, A. Thaler, N. Ni, S.L. Bud'ko, P.C. Canfield, J. Schmalian, R.J. McQueeney, and A.I. Goldman, *Phys. Rev. Lett.* **104**, 057006 (2010).
- [25] E.G. Moon and S. Sachdev, *Phys. Rev. B* **85**, 184511 (2012).
- [26] R.M. Fernandes and J. Schmalian, *Supercond. Sci. Technol.* **25**, 084005 (2012).
- [27] R.M. Fernandes, S. Maiti, P. Wölfle, and A.V. Chubukov, *Phys. Rev. Lett.* **111**, 057001 (2013).
- [28] C. Platt, R. Thomale, C. Honerkamp, S.-C. Zhang, and W. Hanke, *Phys. Rev. B* **85**, 180502(R) (2012).
- [29] M. Khodas and A.V. Chubukov, *Phys. Rev. Lett.* **108**, 247003 (2012).
- [30] T. Das and A.V. Balatsky, [arXiv:1208.2468](https://arxiv.org/abs/1208.2468).
- [31] V. Stanev and Z. Tesanović, *Phys. Rev. B* **81**, 134522 (2010).
- [32] T. Shimojima, F. Sakaguchi, K. Ishizaka, Y. Ishida, T. Kiss, M. Okawa, T. Togashi, C.-T. Chen, S. Watanabe, M. Arita, K. Shimada, H. Namatame, M. Taniguchi, K. Ohgushi, S. Kasahara, T. Terashima, T. Shibauchi, Y. Matsuda, A. Chainani, and S. Shin, *Science* **332**, 564 (2011).
- [33] J.-Ph. Reid, M.A. Tanatar, A. Juneau-Fecteau, R.T. Gordon, S.R. de Cotret, N. Doiron-Leyraud, T. Saito, H. Fukazawa, Y. Kohori, K. Kihou, C.H. Lee, A. Iyo, H. Eisaki, R. Prozorov, and L. Taillefer, *Phys. Rev. Lett.* **109**, 087001 (2012); J.-Ph. Reid *et al.*, *Supercond. Sci. Technol.* **25**, 084013 (2012).
- [34] K. Okazaki *et al.*, *Science* **337**, 1314 (2012).
- [35] J.T. Park, G. Friemel, Y. Li, J.-H. Kim, V. Tsurkan, J. Deisenhofer, H.-A. Krug von Nidda, A. Loidl, A. Ivanov, B. Keimer, and D.S. Inosov, *Phys. Rev. Lett.* **107**, 177005 (2011); G. Friemel, J.T. Park, T.A. Maier, V. Tsurkan, Y. Li, J. Deisenhofer, H.-A. Krug von Nidda, A. Loidl, A. Ivanov, B. Keimer, and D.S. Inosov, *Phys. Rev. B* **85**, 140511(R) (2012).
- [36] M. Xu, Q.Q. Ge, R. Peng, Z.R. Ye, J. Jiang, F. Chen, X.P. Shen, B.P. Xie, Y. Zhang, A.F. Wang, X.F. Wang, X.H. Chen, and D.L. Feng, *Phys. Rev. B* **85**, 220504(R) (2012).
- [37] G.S. Tucker, D.K. Pratt, M.G. Kim, S. Ran, A. Thaler, G.E. Granroth, K. Marty, W. Tian, J.L. Zarestky, M.D. Lumsden, S.L. Bud'ko, P.C. Canfield, A. Kreyssig, A.I. Goldman, and R.J. McQueeney, *Phys. Rev. B* **86**, 020503 (R) (2012).
- [38] F. Kretzschmar, B. Muschler, T. Boöhm, A. Baum, R. Hackl, H.-H. Wen, V. Tsurkan, J. Deisenhofer, and A. Loidl, *Phys. Rev. Lett.* **110**, 187002 (2013).
- [39] G. Livanas, A. Aperis, P. Kotetes, and G. Varelogiannis, [arXiv:1208.2881](https://arxiv.org/abs/1208.2881).
- [40] See Supplemental Material at <http://link.aps.org/supplemental/10.1103/PhysRevLett.111.127001> for derivation of the free energy and details of the Eliashberg calculation.
- [41] R.M. Fernandes and J. Schmalian, *Phys. Rev. B* **82**, 014521 (2010).
- [42] S. Maiti and A.V. Chubukov, *Phys. Rev. B* **87**, 144511 (2013).
- [43] M. Yoshizawa, D. Kimura, T. Chiba, A. Ismayil, Y. Nakanishi, K. Kihou, C.-H. Lee, A. Iyo, H. Eisaki, M. Nakajima, and S. Uchida, *J. Phys. Soc. Jpn.* **81**, 024604 (2012).
- [44] L.R. Testardi, in *Physical Acoustics*, edited by W.P. Mason and R.N. Thurston (Academic, New York, 1973).
- [45] A.J. Millis and K.M. Rabe, *Phys. Rev. B* **38**, 8908 (1988).
- [46] F.F. Tafti, A. Juneau-Fecteau, M.-E. Delage, S. Rene de Cotret, J.-Ph. Reid, A.F. Wang, X.-G. Luo, X.H. Chen, N. Doiron-Leyraud, and L. Taillefer, *Nat. Phys.* **9**, 349 (2013).
- [47] H.-H. Kuo, J.G. Analytis, J.-H. Chu, R.M. Fernandes, J. Schmalian, and I.R. Fisher, *Phys. Rev. B* **86**, 134507 (2012).
- [48] M. Sgrist, *Prog. Theor. Phys.* **107**, 917 (2002).
- [49] M.B. Walker and P. Contreras, *Phys. Rev. B* **66**, 214508 (2002).
- [50] T.A. Maier, P.J. Hirschfeld, and D.J. Scalapino, *Phys. Rev. B* **86**, 094514 (2012).